

Causality Enforcement in Transient Simulation of Passive Networks through Delay Extraction

Rohan Mandrekar¹, Madhavan Swaminathan²
 School of Electrical and Computer Engineering
 Georgia Institute of Technology
 Atlanta GA 30332-0250

Email: rohan¹,madhavan.swaminathan²@ece.gatech.edu

Abstract

Causality, which deals with the precise timing of signal propagation through passive structures like interconnects, is an important problem in the time domain simulation of distributed passive networks. If unaccounted for, it can lead to significant error in the signal integrity analysis of high-speed digital systems. This paper demonstrates the enforcement of causality on the transient simulation of distributed passive networks based on the extraction of the port-to-port delay. The paper describes a technique to extract the port-to-port delay in passive networks directly from their frequency domain response. The technique can be applied to either S, Y or Z parameters of passive networks and can be extended to multi-port and mixed mode networks.

1. Introduction

The advances in high performance digital systems in terms of both speed and complexity have necessitated accurate and faster transient simulation techniques. The fundamental difficulty encountered in such transient simulations is that passive structures by themselves are analyzed in the frequency domain while their terminations are often nonlinear devices like drivers and receivers which can only be analyzed in the time domain. This requires sound techniques to accurately transform the frequency response data of passive structures to the time domain to perform transient simulation. The simplest way to transform frequency domain data to the time domain is through the Inverse Fourier Transform [1]. According to the Inverse Fourier Transform, a passive frequency domain response can be transformed into a stable time domain response subject to the causality condition which forces the time domain response to be zero for $t < 0$. However with increasing clock frequencies, the size of the passive structures is comparable to the signal wavelength at the operating frequency, leading to distributed effects like delay playing an important role in the time domain analysis. These distributed effects imply that there are many causality condi-

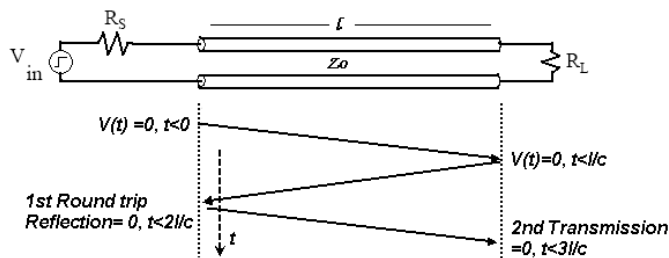


Figure 1: Multiple causality conditions on a transmission line response

tions that need to be satisfied, to generate the correct signal response in the time domain [2]. Figure 1 shows the multiple causality conditions due to the finite velocity of the electromagnetic waves propagating on a transmission line. Present frequency domain macro-modeling techniques analyze a passive structure in the frequency domain and then approximate the bandlimited frequency response using lumped elements. However such representations of passive structures are unable to accurately capture the distributed effects since the data obtained from frequency domain analysis is bandlimited and without explicit information on the delay embedded in the systems. Other existing techniques like the W-element models for transmission lines in HSPICE simulate causality conditions well. However these models are not applicable to arbitrary passive structures [2]. This often leads to the violation of the causality conditions in the transient simulation of passive networks. An example of such a case is shown in Figure 2 where the circuit shown in figure 1 was simulated using bandlimited frequency response data of the transmission line. The source and load impedances were left mismatched in order to generate reflections. Such violations of causality can considerably affect the signal integrity analysis in high-speed systems [3]. Since the port-to-port delay in a passive system is the basis for these causality conditions (Figure 1), determination of this delay from the frequency domain response enables the enforcement of causality on the transient simulations.

2. Causality violation in bandlimited modeling of passive networks

Macro-modeling of a passive network involves development of a black-box representation of the network which approximates its port-to-port behavior [4]. Such a representation is generated by approximating the frequency response of the net-

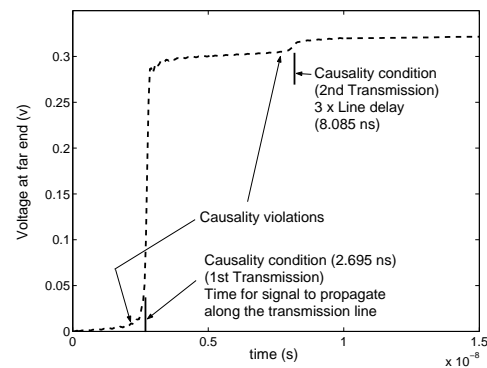


Figure 2: Transmission line transient simulation violating causality

work using complex poles and residues in the form

$$H(s) = \sum_{n=1}^N \frac{\alpha_n}{s - \beta_n} + k_d + k_l s \quad (1)$$

where β_n are the complex poles, α_n are the complex residues and $s = j\omega$ where ω is the angular frequency. Once the poles and residues are known, they can be represented in a lumped-element-circuit form to be used in SPICE. $H(s)$ generated this way is stable if all the poles β_n lie in the left half of the complex s-plane. To ensure passivity of $H(s)$ several methods have been proposed in literature. For instance, the one described in [4] imposes a set of conditions on the residues α_n , k_d and k_l , to ensure that the developed macro-model is passive. Macro-models developed using such techniques satisfy the stability and passivity criteria, but not causality. This is because distributed passive systems have infinite poles, and equation 1 approximates their response using only a finite number of poles N , obtained using bandlimited frequency response data. This prevents $H(s)$ from accurately capturing the delay in the network, since capturing delay using a function in the pole-residue form shown in equation 1 would require an infinite number of poles N .

3. Delay extraction from frequency domain data

Passive networks simply absorb, transfer and dissipate electrical energy provided to them and are limited by their inability to amplify signals. This results in passive responses having minimum phase which can be used to extract delay embedded in these networks. To understand the concept of minimum phase [1] consider a one-port passive network with impedance parameter $Z11(s)$ where $s = j\omega$ and ω is the angular frequency. If the system is stable then all the poles of $Z11(s)$ lie in the left half of the complex s-plane. Now the same system can also be represented using admittance parameter $Y11(s)$ where $Y11(s) = 1/Z11(s)$. Since the system is stable, all the poles of $Y11(s)$ also lie in the left half of the complex s-plane. However, since the poles of $Y11(s)$ are the zeros of $Z11(s)$ and vice-versa, all the poles and zeros of $Z11(s)$ and $Y11(s)$ lie in the left half of the complex s-plane. This property constrains the phase response of the system such that $-\pi < \angle Z11(s) < \pi$ and $-\pi < \angle Y11(s) < \pi$. Such a system is called a minimum phase system and $Z11(s)$ and $Y11(s)$ are called minimum phase functions. The phase response of such functions does not show any phase transition.

In multi-port passive networks, this property of minimum phase is observed only for the self-responses i.e., only for the diagonal elements of the system matrix. Consider a 2-port passive network represented using impedance parameters

$$Z(s) = \begin{bmatrix} Z11(s) & Z12(s) \\ Z21(s) & Z22(s) \end{bmatrix} \quad (2)$$

In this system only $Z11(s)$ and $Z22(s)$ are minimum phase functions. The transfer impedances $Z12(s)$ and $Z21(s)$ are stable but do not exhibit minimum phase. This is because of the port-to-port delay embedded in these transfer impedance responses. Let Td be the delay between ports 1 and 2 in the above system. Then $Z12(s)$ can be written as

$$Z12(s) = Z12'(s)e^{-sTd} \quad (3)$$

According to linear system theory [1] any stable system function can be represented as a product of a minimum phase function and an all-pass function, where an all-pass function is one whose magnitude is unity over the entire frequency range. Therefore

$$Z12(s) = Z12_{\min}(s) \cdot Z12_{AP}(s) \quad (4)$$

Comparing equations 3 and 4 and noting that e^{-sTd} has unity magnitude, it can be seen that if $Z12(s)$ is separated into a product of a minimum phase function and an all-pass function, the all-pass function will represent the delay between the two ports. This separation can be performed using the Hilbert Transform [1].

The Hilbert Transform relates the magnitude and phase of a minimum phase function $H_{\min}(j\omega)$ through the equation

$$\arg[H_{\min}(j\omega)] = -\frac{1}{2\pi} P \int_{-\pi}^{\pi} \log |H_{\min}(j\theta)| \cot\left(\frac{\omega - \theta}{2}\right) d\theta \quad (5)$$

where P is the Cauchy Principal value. Since an all-pass function has unity magnitude, the magnitude response of the minimum phase function $Z12_{\min}(s)$ in equation 4 is the same as that of $Z12(s)$. Therefore the port-to-port delay Td embedded in the transfer impedance parameter $Z12(s)$ can be determined as follows

$$|Z12_{\min}(j\omega)| = |Z12(j\omega)| \quad (6)$$

$$\arg[Z12_{\min}(j\omega)] = -\frac{1}{2\pi} P \int_{-\pi}^{\pi} \log |Z12(j\theta)| \cot\left(\frac{\omega - \theta}{2}\right) d\theta \quad (7)$$

$$Z12_{AP}(j\omega) = \frac{Z12(j\omega)}{Z12_{\min}(j\omega)} = e^{-j\omega Td} \quad (8)$$

$$Td = -\frac{\arg(Z12_{AP}(j\omega))}{\omega} \quad (9)$$

This technique can be used to determine the delay from the S, Y or Z parameter representation of a passive system.

To demonstrate the proposed technique, a power/ground PCB plane pair was analyzed using the cavity resonator method [5] to obtain the Z-parameter representation. The plane pair was 25cm x 25cm with 8mil separation and the two ports under consideration were located at (1.67,2.33)cm and (22.67,2.33)cm respectively. Using the velocity of propagation of electromagnetic waves in a dielectric medium, the delay between the two ports was found to be about 1.5ns. Next, the technique previously described in this section was used to determine the delay between the two ports. Starting with the Z-parameters, Figures 3 and 4 show the comparison between the magnitude and phase responses of $Z11$ and $Z12$. From the phase response, it can be easily inferred that $Z11$ is a minimum phase response as against $Z12$ which has 2 phase transitions. Using equations 6 through 8 $Z12$ was separated into a minimum phase function $Z12_{\min}$ and an all-pass function $Z12_{AP}$. The magnitude and phase responses for $Z12_{\min}$ and $Z12_{AP}$ are shown in Figures 5 and 6. Since $Z12_{AP}$ is of the form e^{-sTd} the port-to-port delay Td can be computed as the negative gradient of the phase of $Z12_{AP}$. The minor deviations from the ideal magnitude and

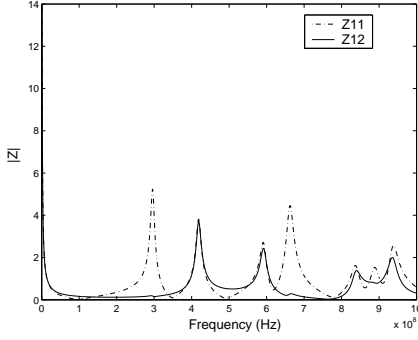


Figure 3: Z-parameter magnitude response for the plane

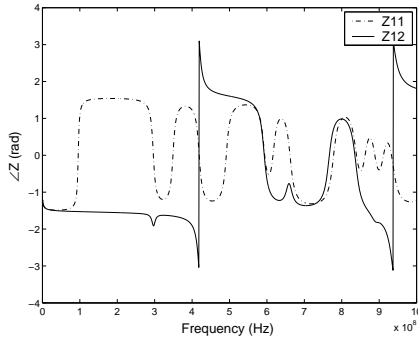


Figure 4: Z-parameter phase response for the plane

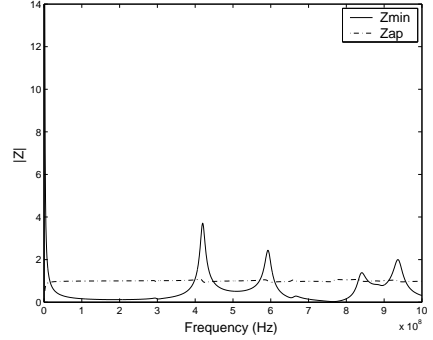


Figure 5: Magnitude response for $Z_{12_{min}}$ and $Z_{12_{AP}}$

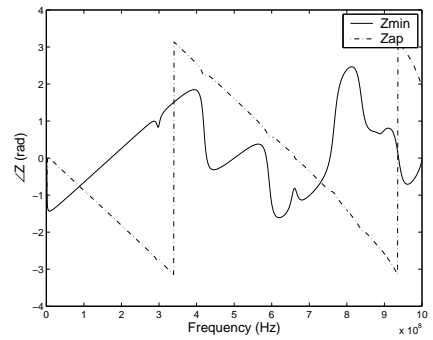


Figure 6: Phase response for $Z_{12_{min}}$ and $Z_{12_{AP}}$

phase responses of $Z_{12_{AP}}$ seen in Figures 5 and 6 can be eliminated by averaging. The delay thus determined was found to be 1.517ns, which is in good agreement with the expected value.

As another demonstration of the delay extraction technique, 4-port S-parameter measurements of various differential transmission line structures were processed to extract their respective delays. For mixed mode structures, the scattering parameters are first transformed into mixed mode parameters followed by their separation into minimum phase and all-pass components to get even and odd mode delays. The extracted delay values were compared with the delays observed using the TDT waveform computed through Agilent's PLTS system. The comparison chart is shown in Table 1.

4. Causality enforcement using delay extraction

The port-to-port delay extracted using the procedure described in the previous section can be used to enforce causality on the transient simulation. Most transient simulators that directly incorporate the scattering (or impedance) parameters of a multi-port passive network perform the transient simulation using a convolution integration technique [6]. This involves

the computation of the impulse responses of the network followed by their convolution with input signals. For the circuit shown in Figure 1 the transient simulation was carried out using a signal flow graph shown in Figure 7. Since the port-to-port delay for the above network had been estimated directly from the frequency data, the computed transfer impulse responses could be compensated such that the delay in network was accurately captured. This was done by forcing the transfer impulse responses $s_{12}(t)$ and $s_{21}(t)$ to zero over the delay period. The compensated impulse responses were transformed back to the frequency domain to check for any passivity violation. It was observed that the causality compensation carried out on the transfer impulse responses of the passive network did not violate its passivity. The transient simulation results with causality enforced are shown in Figure 8. It can be clearly seen that the transient simulation satisfies all causality conditions.

To understand the effect of causality violations on the accuracy of a transient simulation and the resulting impact on signal integrity analysis, the transmission line system in Figure 1 was excited by a 3.33 GHz random bit pattern source with a 100 ps rise time. The transient response across the load impedance

	Measured		Extracted	
	Even	Odd	Even	Odd
Microstrip	230ps	239ps	230.5ps	236.8ps
Stripline	247ps	247ps	243.3ps	242.6ps
Buried microstrip	229ps	240ps	227.7ps	237ps

Table 1: Delay extraction for differential transmission lines

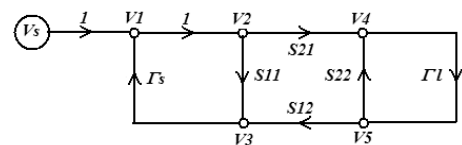


Figure 7: Signal flow graph for the transmission line system

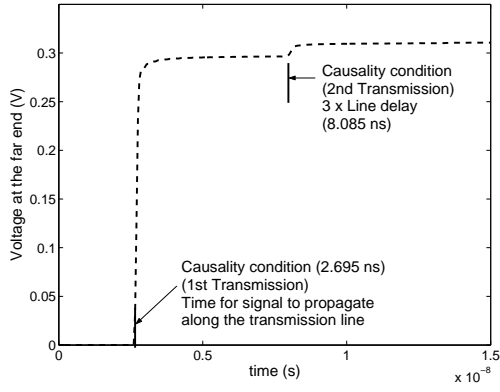


Figure 8: Transmission line transient simulation with causality enforced

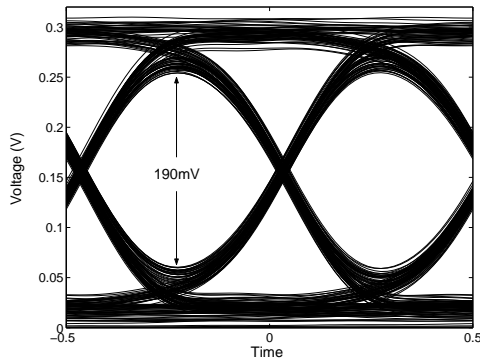


Figure 9: Eye-diagram without causality compensation

was simulated for two cases and the results were represented using eye-diagrams. The eye-diagram obtained from the transient simulation using no causality compensation is shown in Figure 9. The eye-diagram obtained using causality compensation is shown in Figure 10. The x - axis in the eye-diagrams spans a time period of 300ps. It can be readily seen that the eye opening in Figure 9 (190 mV) is much smaller than that in Figure 10 (220 mV). This indicates that causality violations can significantly compromise the accuracy of a transient simulation.

An additional advantage gained from the estimation of the port-to-port delay in a transient simulation is the ability to par-

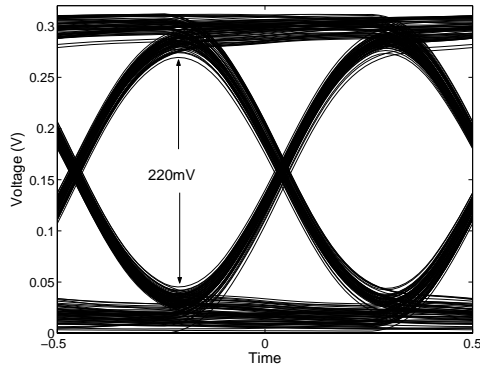


Figure 10: Eye-diagram with causality compensation

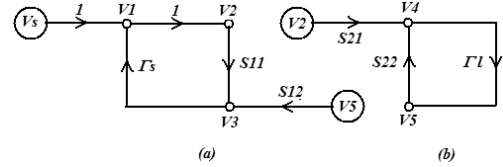


Figure 11: Separation of signal flow graph into sub-graphs

tion circuits and perform the simulation in a distributed fashion. For the transmission line circuit considered in this paper, it is known from the signal flow graph in Figure 7 that the voltage V_2 does not reach V_4 (and V_5 does not reach V_3) for a time period given by the port-to-port delay. This means that $s_{12}(t)$ and $s_{21}(t)$ are zero over that initial period forcing the corresponding convolution integrals to zero over that time. This can be used to re-write the convolution equations for V_4 and V_3 as

$$V_3(t) = V_2(t) \otimes s_{11}(t) + V_5(t - Td) \otimes s'_{12}(t) \quad (10)$$

$$V_4(t) = V_2(t - Td) \otimes s'_{21}(t) + V_5(t) \otimes s_{22}(t) \quad (11)$$

where $s'_{12}(t)$ and $s'_{21}(t)$ are the transfer impulse responses of the transmission line after the delay portion has been removed. Since $V_5(t - Td)$ and $V_2(t - Td)$ are known at time t , this enables the division of the original signal flow graph into two smaller subgraphs shown in Figure 11 which can be simulated in a distributed fashion. Such circuit partitioning can be useful in reducing simulation time when dealing with multi-port networks with a large number of ports and complex drivers and receivers attached at various ports.

Conclusion

Causality is an important problem in transient simulation of distributed passive networks and causality violations can significantly compromise the accuracy of transient simulations. Since the port-to-port delay forms the basis for the causality conditions in distributed passive networks, the determination of this delay enables the enforcement of causality on the transient simulations. Additionally, it also enables the partitioning of the circuit to aid distributed simulation for larger problems.

References

- [1] Oppenheim, A. and Schaffer, R., *Discrete-time Signal Processing*, 2nd ed. Prentice Hall, 1999, Ch 5,11.
- [2] Kim, W. and Swaminathan, M., "Validity of non-physical RLGC models for simulating lossy transmission lines", Proceedings of the ISAP, Vol.3, 2002. pp 786-789.
- [3] Kim, W., "Development of measurement based time-domain models and its application to wafer level packaging", Ph.D Thesis, ECE, Georgia Tech, 2004 Ch 1,3.
- [4] Min, S. and Swaminathan, M., "Efficient construction of passive macromodels for resonant networks", Proceedings of 10th EPEP, Aug, 2001. pp 229-232
- [5] Chun, S., "Methodologies for modeling simultaneous switching noise in multi-layered packages and boards", Ph.D Thesis, ECE, Georgia Tech.
- [6] Agilent Advanced Design System, User Manual, "Transient and Convolution Simulation"